Applied Surface Science 264 (2013) 261–268

Contents lists available at SciVerse ScienceDirect

Applied Surface Science

journal homepage: www.elsevier.com/locate/apsusc

Effects of acid treatment on structure, properties and biocompatibility of carbon nanotubes

Chenbo Dong[a], Alan S. Campell[a], Reem Eldawud[a], Gabriela Perhinschi[a], Yon Rojanasakul[b], Cerasela Zoica Dinu[a,*]

[a] Department of Chemical Engineering, West Virginia University, Morgantown, WV 26506, USA
[b] Department of Basic Pharmaceutical Sciences, West Virginia University, Morgantown, WV 26506, USA

ARTICLE INFO

Article history:
Received 28 July 2012
Received in revised form
25 September 2012
Accepted 28 September 2012
Available online 23 October 2012

Keywords:
Nanotubes
Acid treatment
Structure modification
Cytotoxicity
Biocompatibility

ABSTRACT

Carbon nanotubes (CNTs) are promising to be the next generation of viable tools for bioapplications. Further advances in such bioapplications may depend on improved understanding of CNTs physical and chemical properties as well as control over their biocompatibility. Herein we performed a systematic study to show how acid oxidation treatment changes CNTs physical and chemical properties and leads to improved CNTs biocompatibility. Specifically, by incubating CNTs in a strong acid mixture we created a user-defined library of CNTs samples with different characteristics as recorded using Raman energy dispersive X-ray spectroscopy, atomic force microscopy, or solubility tests. Systematically characterized CNTs were subsequently tested for their biocompatibility in relation to human epithelial cells or enzymes. Such selected examples are building pertinent relationships between CNTs biocompatibility and their intrinsic properties by showing that acid oxidation treatment lowers CNTs toxicity providing feasible platforms to be used for biomedical applications or the next generation of biosensors.

1. Introduction

Carbon nanotubes (CNTs) are nanoscale diameter materials of tubular shape and micrometer length with many interesting properties that make them viable candidates for a wide range of applications including electrical circuits [1], hydrogen storage [2], fiber optics [3], and conductive plastics [4]. In recent years, CNTs functionalization with biomolecules such as proteins [5], enzymes [6,7] or nucleic acids [8] opened up exciting bioapplications in biolabeling [9], biosensing [10], drug delivery [11], bioseparation [12] and tissue engineering [13]. However, further development of such bioapplications is hindered by: (1) CNT's limited available surface area for biomolecule functionalization [14], (2) lack of understanding of CNTs growth mechanisms in uncontaminated forms [15], (3) CNTs structural instability since larger nanotubes are prone to kinking and collapsing [16,17], and (4) CNTs cytotoxicity and associated health risks posed during their manufacturing and processing [18]. These challenges are mainly associated with the fact that as-produced CNTs form large aggregates in liquid enviroments since their hydrophobic walls are prone to van der Waals interactions [19]. Thus, in order to increase CNTs bioapplications [20] and reduce their aggregation [21] and cytotoxicity [22], it is critical to overcome their intrinsic hydrophobicity and tendency to form conglomerates in solution.

Numerous attempts have been made to overcome CNTs hydrophobicity and increase their hydrophilicity; these include gas- [23] and liquid-phase activation [24], and oxidation with strong oxidants including hydrogen peroxide [25], potassium permanganate [26], potassium hydroxide [27], and nitric and/or sulfuric acid [6,7,28]. Among these attempts, nitric and sulfuric acid oxidation is regarded as the most prevalent treatment since it is easy to implement in both laboratory and industrial settings [20]. When CNTs are oxidized with such aggressive acids, their hydrophilicity is increased by the introduction of oxygen-containing functional groups, i.e., carboxyl [29], carbonyl [26,29], and phenol groups [30]. Moreover, during such oxidation treatments amorphous carbon [31] and residual metal catalyst particles are removed, possibly resulting in reduced intrinsic toxicity of CNTs [22]. Despite the fact that wide evaluations of the effects of acid oxidation on CNTs have been carried out, systematic investigations of changes in physical and chemical properties and how such changes can be further employed for increasing CNTs biocompatibility and thus bioapplications are still lacking.

Herein we performed a systematic study of the changes in physical and chemical properties of pristine CNTs upon user-controlled

* Corresponding author at: Department of Chemical Engineering, West Virginia University, Benjamin M. Statler College of Engineering and Mineral Resources, PO Box 6102, Morgantown, WV 26506, USA. Tel.: +1 304 293 9338; fax: +1 304 293 4139.
E-mail address: cerasela-zoica.dinu@mail.wvu.edu (C.Z. Dinu).

0169-4332/$ – see front matter © 2012 Elsevier B.V. All rights reserved.
http://dx.doi.org/10.1016/j.apsusc.2012.09.180

treatment with nitric and sulfuric acids. Further, we assessed how these changes affect CNTs biocompatibility in relation to cellular and enzymatic systems [6,7,10]. Our hypothesis was that selected biological examples will help build pertinent relationships between CNTs biocompatibility and their intrinsic properties and demonstrate how interface reactions between a biological molecule and the nanomaterial can be further used to provide systems with lower toxicity to be used for selected bioapplications as well as feasible platforms for the next generation of biosensors.

2. Materials and methods

2.1. Acid oxidation of CNTs

Acid oxidation treatment of single- and multi-walled carbon nanotubes (SW- and MWCNTs, respectively) was employed to generate a library of samples with different physical and chemical properties. Specifically, commercial SWCNTs (85% purity, Unidym Inc.) and MWCNTs (95% purity, Nanolab Inc. (PD15L5-20)) were incubated in a concentrated sulfuric (96.4%, Fisher, USA) and nitric acid (69.5%, Fisher, USA) mixture in a ratio of 3:1 (V/V). The CNTs/acids mixture (where CNTs can refer to either SW- or MWCNTs) was subsequently sonicated in an ice bath (Branson 2510, Fisher, USA) for 1, 3, or 6 h, at a constant temperature of 23 °C. When the required time elapsed, CNTs/acids mixture was diluted with deionized (di) water and filtered through a GTTP 0.2 μm polycarbonate filter membrane (Fisher, USA). Several cycles of resuspension in di water were employed to remove acidic residues or catalysts. The CNTs were isolated on the filter, subsequently dried in a vacuum desiccator and stored at room temperature for further use.

2.2. Energy dispersive X-ray analysis (EDX) of CNTs

Energy dispersive X-ray analysis (EDX) was used for quantitative elemental analysis of pristine and acid oxidized CNTs. Samples (1 mg/ml in di water) were deposited on silica wafers and dried under vacuum. The experiments were performed on a Hitachi S-4700 Field Emission Scanning Electron Microscope (USA) with a S-4700 detector combining secondary (SE) and backscattered (BSE) electron detection (all in a single unit), operating at 20 kV. Results are presented as a percent of elements relative to the most dominant element.

2.3. Scanning Electron Microscopy (SEM) of CNTs

Samples (1 mg/ml in di water of both pristine and acid treated CNTs) were dried on silica wafers under vacuum and imaged using a Hitachi S-4700 Field Emission Scanning Electron Microscope (USA) with a field emission at 10 kV.

2.4. Raman spectroscopy of CNTs

Raman spectroscopy (performed on a Renishaw InVia Raman Spectrometer, CL532-100, 100 mW, USA) allowed determination of the chemical structure and any modifications resulted from the acids oxidation of both pristine and acids treated CNTs. Briefly, CNTs deposited on glass slides (Fisher, USA) were excited through a 20× microscope objective using an Argon ion (Ar^+) laser beam with a spot size of <0.01 mm^2 operating at 514.5 nm. Detailed scans were taken in the 100–3200 cm^{-1} range; low laser energy (i.e., <0.5 mV) and exposure time of 10 s were used to prevent unexpected heating effects.

2.5. CNTs solubility measurement

The solubility of CNTs (pristine and acids oxidized) was evaluated in di water (pH 6.25) and Phosphate Saline Buffer (PBS, pH 7, 100 mM ionic strength). Briefly, CNTs were diluted in the solvent of interest to yield to a 3 mg/ml solution. The suspension was then centrifuged at 3000 rpm for 5 min; subsequently, part of the supernatant (0.8 ml) was removed and filtered through a 0.2 μm GTTP filter membrane. The filter membrane was then dried under vacuum and the amount of CNTs was weighted. The solubility of the CNTs was calculated based on the volume used for suspension and the initial starting amount.

2.6. CNTs length measurement

An atomic force microscope (AFM, Asylum Research, USA) was used to evaluate the length of pristine and acids treated CNTs. A Si tip (Asylum Research, 50–90 kHz AC240TS, USA) helped perform tapping mode in air. CNTs samples (i.e., pristine, 1, 3 or 6 h acids oxidized SW and MWCNTs) were dispersed in di water (to yield solutions of 0.1 mg/ml concentration), deposited on mica surfaces (9.5 mm diameter, 0.15–0.21 mm thickness, Electron Microscopy Sciences, USA) and allowed to dry over night under vacuum. Scan images of 10, 5 or 1 (μm × μm) areas were acquired. For each sample, at least 30 individual CNTs were counted and measured to obtain average length distribution.

2.7. Cell culture and treatment with CNTs

Non-tumorigenic human bronchial epithelial cells (BEAS-2B) were purchased from American Type Culture Collection (ATCC, USA). The cells were cultured in DMEM medium supplemented with 5% fetal bovine serum (FBS), 2 mM L-glutamine and 100-units/ml penicillin/streptomycin (all reagents were purchased from Invitrogen, USA). Cells were passaged weekly using 0.05% trypsin (Invitrogen, USA) and kept in 5% CO_2 at 37 °C.

Pristine and acids oxidized SWCNTs were dispersed in di water by sonication, filtered through the 0.2 μm GTTP filter membrane, resuspended in cellular media and sonicated at room temperature to form stable dispersions. For treatment, BEAS-2B cells were seeded overnight in a 12 well plates (Fisher, USA) at a density of 3.5E5 cells/well, and allowed to reach confluence. Subsequently, the cells were exposed to 100 μg/ml SWCNTs; 24 h post exposure, the cells were incubated with 6.5 μg/ml Hoechst 33342 dye (Molecular Probes, USA) for 30 min at 37 °C and analyzed for apoptosis by scoring the percentage of cells with intensely condensed chromatin and/or fragmented nuclei using fluorescence microscopy (Leica Microsystems, USA). Approximately 1000 cell nuclei from ten random fields were analyzed for each sample. The apoptotic index was calculated as the percentage of cells with apoptotic nuclei relative to the total number of cells. At least 3 independent trials were performed for each sample.

2.8. Functionalization of CNTs with enzyme

Soybean peroxidase (SBP, Bioresearch, USA) was covalently attached to 1, 3 or 6 h acid treated MWCNTs using 1-ethyl-3-[3-dimethylaminopropyl] carbodiimide hydrochloride (EDC; Acros Organics, USA) and N-hydroxysuccinimide (NHS, Pierce, USA) [32]. Briefly, 2 mg CNTs (MWCNTs) were dispersed in 160 mM EDC and 80 mM NHS (total volume of 2 ml in MES (2-(N-morpholino)ethanesulfonic acid sodium salt, 50 mM, pH 4.7, Sigma, USA) for 15 min at room temperature with shaking at 200 rpm. The activated MWCNTs were next filtered through the 0.2 μm GTTP filter membrane, washed thoroughly with MES buffer to remove any ester residues, immediately dispersed in 2 ml of 1 mg/ml SBP

solution in PBS (100 mM, pH 7.0) and incubated for 3 h at room temperature at room temperature with shaking at 200 rpm. The resulting SBP–MWCNT conjugates were filtered and washed extensively with PBS to remove any unbound enzyme [32]. The supernatants and washes were collected to quantify enzyme loading.

2.9. Enzyme loading

The amount of SBP attached to MWCNTs (i.e., SBP loading) was determined using standard BCA assay kit (Pierce, USA) and subtracting the amount of enzyme washed out in the supernatant and washes from the amount of SBP initially added to the MWCNTs. Briefly, the working reagent (1000 μl) was prepared by mixing 50 parts of reagent A with 1 part of reagent B (the reagents are provided with the kit). The mixture of reagents A and B was further added to 50 μl solutions of SBP-containing samples (i.e., the samples isolated in the form of the supernatant and washes). The resulting solutions were incubated at 37 °C for 30 min. Absorbance at 562 nm was determined on a spectrophotometer (Fisher, USA). Control calibration curves were prepared by serial dilutions of SBP (free in solution) into the working reagent.

2.10. Enzyme activity assay

The activity of SBP was measured by monitoring the oxidation reaction of (2,2′-Azinobis [3-ethylbenzothiazoline-6-sulfonic acid]) (ABTS, Sigma, USA) in the presence of hydrogen peroxide (H_2O_2, Sigma, USA). 20 μl of the SBP–MWCNTs conjugates were added to 0.65 ml ABTS solution (0.5 mM final concentration, Pierce, USA) and mixed; subsequently, 20 μl H_2O_2 solution (0.2 mM final concentration) was added to the sample in order to initiate the reaction. The change in absorbance was monitored spectrophotometrically at 412 nm immediately upon addition of H_2O_2. The initial reaction rate was calculated from the slope of the linear time-course. The extinction coefficient of the oxidized ABTS product is 32,400 M^{-1} cm^{-1} at 412 nm [33]. The activity of the immobilized enzyme is reported as specific activity relative to free enzyme activity. The activity of the free enzyme was determined using an equivalent amount of free enzyme (based on loading data) and the protocol provided above.

2.11. Statistical analysis

All results are presented as mean ± standard deviation.

3. Results and discussion

We prepared a library of single- and multi-walled carbon nanotubes (SW- and MWCNTs) using liquid phase oxidation with a strong nitric and sulfuric acids mixture [6,7]. The approach is shown in Scheme 1; sonication in the acids mixture attacks the graphene sheets on the C—C bands [34], introduces defects and oxidizes the CNTs at the defect sites leading to shorter nanotubes. To reduce the reaction rate of acids attack, the water bath sonicator was maintained at room temperature. The carboxylic acidic groups introduced in SW- and MWCNTs were determined previously using acid–base titrations [35,36] or the formation of a dodecylamine zwitterions [37].

We further investigated the chemical composition of pristine and acids oxidized CNTs using energy dispersive X-ray analysis (EDX) [20,38]. EDX spectra of pristine SW- and MWCNTs are shown in Fig. 1a and b, respectively, as a plot of X-ray counts vs. energy (in keV). The analysis revealed the presence of high contents of carbon (C) and oxygen (O), with iron (Fe) as metal catalyst in both pristine SW- and MWCNTs samples. The energy peaks correspond to the various elements in the sample, with Fe yielding two peaks at 0.70 keV and 6.40 keV [39]. Other elements (e.g., Al, Si, Cl, S, etc.) were also present but in very low amount. The Fe peak was larger for the SWCNTs sample when compared to the MWCNTs one. The difference was reflective of their pristine characteristics since SWCNTs purity was 85% while the purity of pristine MWCNTs was 95%, per manufacturer information (see Section 2). The insets in Fig. 1 show the changes in the O and Fe contents with the acids oxidation treatment time for both SW- and MWCNTs samples. As shown, Fe content decreased with the treatment time for both SW- and MWCNTs samples indicating removal of the metal catalyst. The decrease in the Fe content was more pronounced for the SWCNTs when compared to MWCNTs samples. This is a reflection of the different purities of the two samples chosen in these experiments. For the O content, the change was also dependent on the sample characteristics. The relative low purity SWCNTs samples contain more amorphous carbon [40] than the higher purity MWCNTs [41]. Thus, the acids treatment led to a significant increase of the O content with the acids treatment time for the SWCNTs (Fig. 1a, inset) when compared to a smaller increase for the MWCNTs samples.

Fig. 2 shows the SEM images of the pristine and acids treated samples (both SW- and MWCNTs). As shown, user-controlled acids treatment did not lead to significant morphological changes either for SW- (Fig. 2a shows pristine SWCNTs while Fig. 2c shows 6 h acids treated SWCNTs) or MWCNTs (Fig. 2c shows pristine MWCNTs while Fig. 2d shows 6 h treated MWCNTs) samples.

The structural changes upon acids treatment of the CNTs samples were investigated using Raman resonance spectroscopy [42–44]. Fig. 3 shows the Raman spectra of pristine and acids treated SW- and MWCNTs. The Raman analysis of the SWCNTs reveals the presence of 4 bands (Fig. 3a), the so-called D (disorder mode) band around 1340 cm^{-1}, G^- and G^+ bands at around 1545 cm^{-1} and 1590 cm^{-1} respectively, and G′ band at 2650 cm^{-1} [22,45]. The Raman analysis of the MWCNTs also reveals the presence of 4 bands (Fig. 3b), with the D band around 1340 cm^{-1}, G band at 1585 cm^{-1}, G′ band at 2650 cm^{-1}, and another band at 2920 cm^{-1} [46,47]. The D band around 1340 cm^{-1} is related to the non-crystalline C species, i.e., defects in the CNTs [48], while the G band observed around 1585 cm^{-1} is indicative of a high degree of ordering and well-structured C-based structures [42]. The size of the D band relative to the G band can be used as a qualitative measurement for the formation of undesired forms of C [49]. Both pristine and acids treated CNTs (SW- and MWCNTs) have a relatively small D band at around 1350 cm^{-1}, with the D band being wider and shifted toward higher frequency in the acids treated

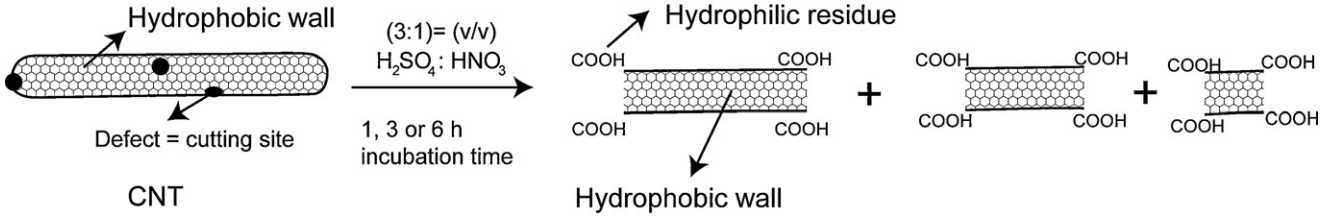

Scheme 1. Time-dependent incubation of pristine CNTs (SW- and MWCNTs) with a mixture of sulfuric and nitric acids leads to acids oxidized CNTs.

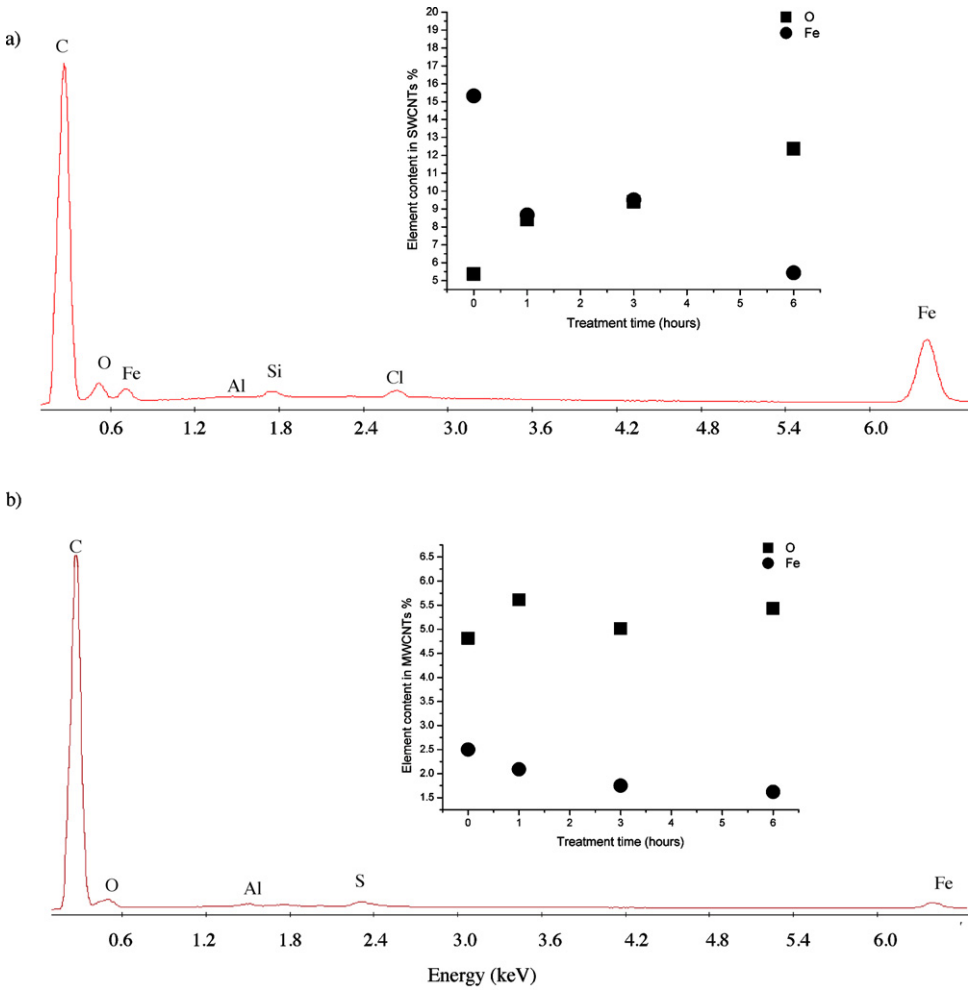

Fig. 1. EDX elemental analysis of pristine SWCNTs (a) and MWCNTs (b). The insets show the changes in the O and Fe contents with the acids treatment time employed under user-control.

samples when compared with the pristine ones. The ratio of intensity of D peak relative to the G peak represents the degree of CNTs functionalization [49]. Higher I_D/I_G ratio suggests higher level of functionalization (I represents the peak's relative intensity).

D band, G band and I_D/I_G ratio of the various CNTs samples (both SW- and MWCNTs) are shown in Table 1. The ratio of I_D/I_G for SWCNTs changed minimally from 0.237 for pristine to 0.263 after 6 h acid treatment. For 1 and 3 h acid oxidized SWCNTs, the I_D/I_G ratio seemed to have decreased. Previous reports have shown that for relatively low purity CNTs (in this particular example the SWCNT's purity is 85%; see Section 2) the I_D/I_G does not provide precise overall information on the sample structure [50], and the I_D/I_G ratio might be both a reflection of washing away amorphous carbon while simultaneously inducing carboxylic acid groups [20].

Table 1
Relative intensity of representative Raman peaks of pristine and acids treated CNTs.

CNT	D band position (cm^{-1})	G band position (cm^{-1})	*ID*/*IG* intensity ratio
Pristine SWCNTs	1328	1590	0.237
1 h cut SWCNTs	1333	1587	0.195
3 h cut SWCNTs	1336	1592	0.229
6 h cut SWCNTs	1336	1595	0.263
Pristine MWCNTs	1345	1586	0.457
1 h cut MWCNTs	1347	1586	0.783
3 h cut MWCNTs	1349	1586	0.788
6 h cut MWCNTs	1351	1589	0.796

For instance, in the initial 1 h SWCNTs acids oxidation, the effect of washing away amorphous C (which is known to lead to decreased I_D/I_G [51]) suppressed the effect of adding carboxylic acid groups (which is known to lead to increased I_D/I_G [52]). However, after 6 h, most of the amorphous C was removed and the I_D/I_G became indicative only of the degree of functionalization with carboxylic groups.

I_D/I_G for MWCNTs increased from 0.457 for pristine to 0.788 for 3 h, and 0.796 after 6 h acids oxidation. This increase in the level of functionalization has a similar trend to the increase in the O or decrease in the Fe catalyst content as observed through the EDX analyses (Fig. 1). Specifically, for the high purity MWCNTs most of the Fe catalysts are removed during the 3 h treatment time (see inset Fig. 1b) this leading to removal of the defects in the MWCNTs structure. Since defects are where the promotion of the carboxylic groups formation takes place [53], and since for the MWCNTs there was a small decrease in the Fe and a small increase in the O content (Fig. 1b inset) from the 3 h to 6 h treatment time, the I_D/I_G for MWCNTs will be minimally changed between these time points as indicated in Table 1. Such analyses confirm that the acids oxidation introduced CNTs chemical property changes i.e., added functional free carboxylic acid groups, to both SW- and MWCNTs sample.

We further investigated how the degree of CNTs dispersion in water-based environments is influenced by the acids oxidation time. We used two solvents with different pH's and ionic strengths, i.e., di water (pH 6.25) and Phosphate Saline Buffer (PBS, pH 7, 100 mM). The results (Fig. 4) indicated that the solubility of CNTs

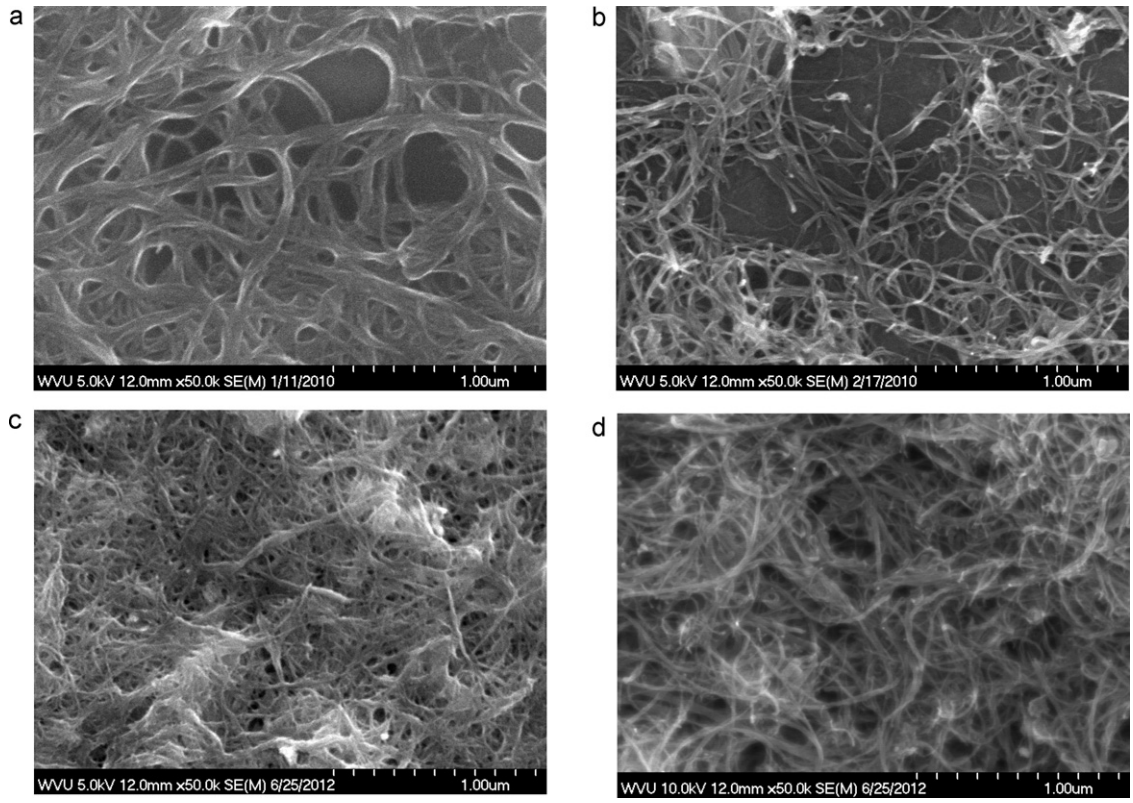

Fig. 2. SEM image of (a) pristine SWCNTs, (b) pristine MWCNTs and (c) 6 h acids treated SWCNTs (d) 6 h acids treated MWCNTs; the scale bar is 1 μm.

in both di water and PBS was improved upon the acids oxidation, with increased acids oxidation times leading to increased solubility. Generally, pristine and acid oxidized SWCNTs (either 1, 3 or 6 h cut) were more dispersed in PBS when compared to di water (Fig. 4a). MWCNTs did not show a similar trend; specifically, pristine and 1 h cut MWCNTs were more soluble in PBS, however, after longer acids oxidation times (i.e., 3 and 6 h) the solubility was higher in water when compared to PBS (Fig. 4b). The changes in the solubility observed for the MWCNTs samples after longer acids oxidation times are correlated with the changes in the functionality of these samples and number of carboxylic acidic groups being generated. Specifically, longer acids oxidation times will lead to higher number of carboxyl groups being generated (see Figs. 1 and 3). When the MWCNTs acids treated samples are placed in water-based environments, carboxylate anions groups are generated by the deprotonation of carboxylic acid groups [54]. At high ionic strength, the probability for these anions to form aggregates [55] increases thus leading to the lower solubility observed for the 3 and 6 h acids oxidized MWCNTs placed in PBS when compared to solubility of these samples placed in water.

Atomic force microscopy (AFM) and tapping mode [56] was used to analyze the morphology and quantify the length of the CNTs samples. Specifically, cross sectional areas from (10×10) to (1×1) μm × μm were scanned to derive the length of at least 30 CNTs/sample (both SW- and MWCNTs; pristine, 1, 3 and 6 h cut). Pristine and acids oxidized CNTs length distributions are shown in

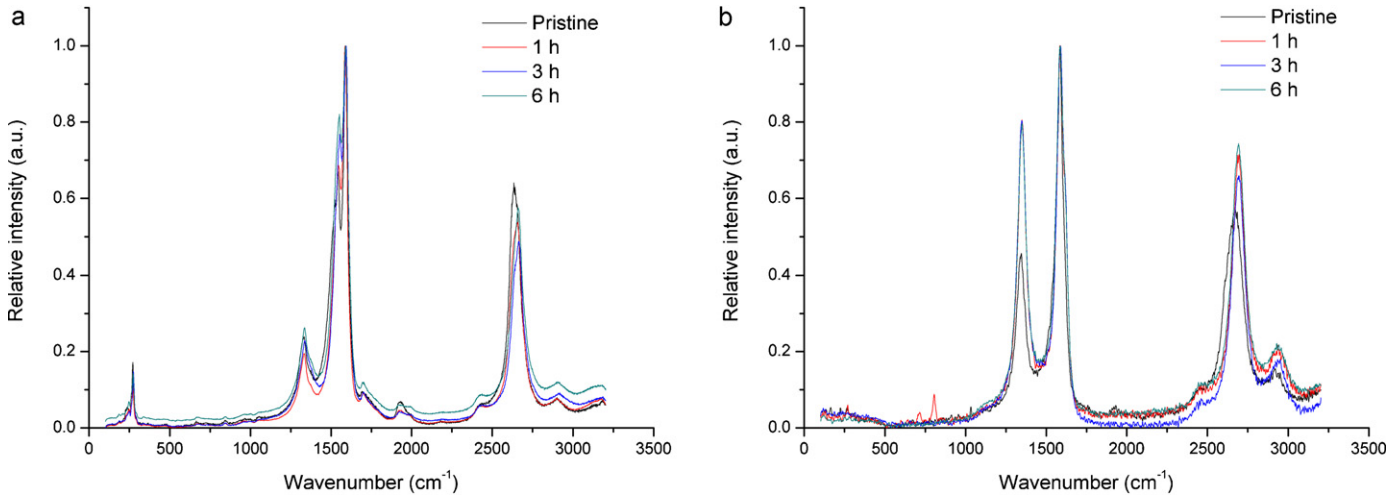

Fig. 3. Raman spectra of pristine, 1, 3 and 6 h acids oxidized SWCNTs (a) and MWCNTs (b).

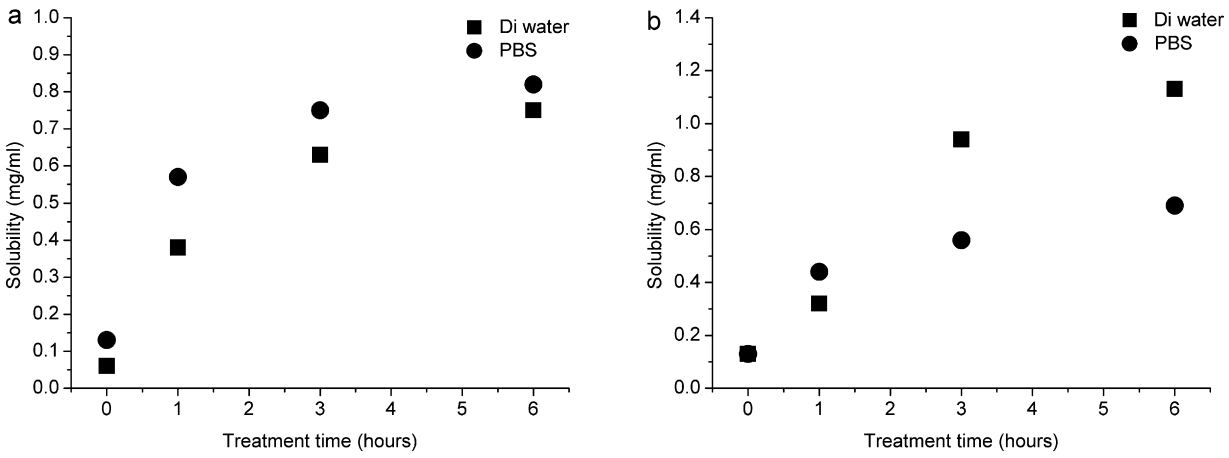

Fig. 4. Solubility of pristine and acids oxidized SWCNTs (a) and MWCNTs (b) in deionized (di) water and phosphate buffer saline (PBS).

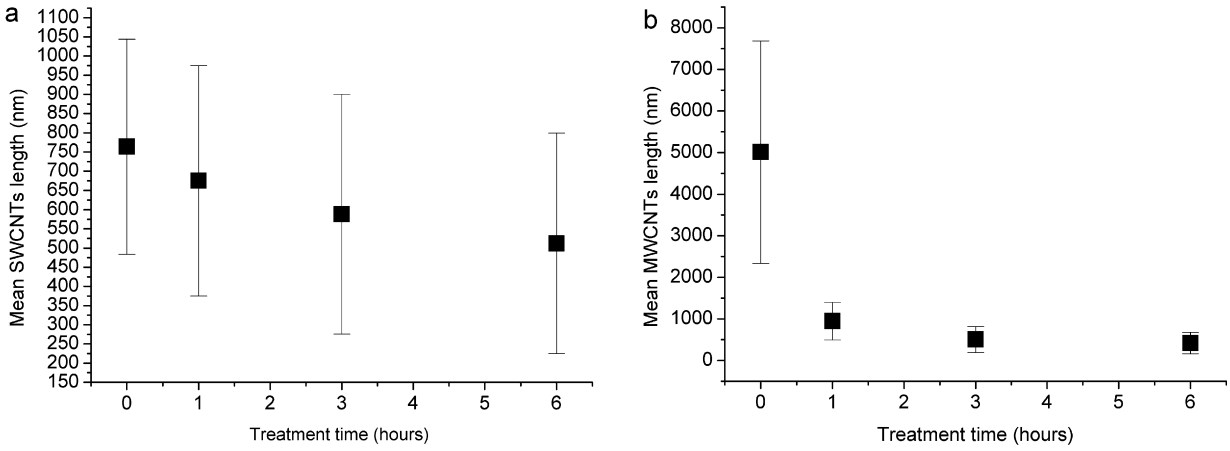

Fig. 5. The average length distribution and the standard deviation of SWCNTs (a) and MWCNTs (b) with the acids treatment time.

Fig. 5; a general non-linear distribution toward shorter CNTs was observed with the increase in the acids oxidation time.

Having established that the acids oxidation influences the chemical and physical properties of pristine CNTs (both SW- and MWCNTs), we proceeded to examine whether user-controlled acids oxidation would also affect CNTs biocompatibility. First, we performed a systematic study on the cellular toxicity resulted from the incubation of immortalized human bronchial epithelial cells with acids oxidized SWCNTs. Previous *in vivo* studies have shown that cellular exposure to SWCNTs results in macrophages without nuclei [57,58], with SWCNTs inducing chromosome aberration [18]. However, to our knowledge, no studies that looked at the influence of the different acids oxidation times to BEAS-2B immortalized human bronchial epithelial cells have been performed. Moreover, to our knowledge, there is no correlation in the literature on how cellular toxicity depends on the SWCNTs physical and chemical properties as impaired by the acids oxidation time and how such toxicity can be controlled. In our experiments, BEAS-2B cells were exposed to SWCNTs for 24–72 h at Permissible Exposure Limit for particulates not otherwise regulated (i.e., 100 μg/ml of SWCNTs, based on previous laboratory exposure levels [58,59]). Fig. 6 shows the percentage of apoptotic BEAS-2B cells upon exposure to SWCNTs; our data shows that the cytotoxicity of the 6 h acids treated SWCNTs is lower than that of pristine SWCNTs. Specifically, the percentage of apoptotic cells for pristine SWCNTs is about 19% while the percentage of apoptotic cells for 6 h acids treated SWCNTs is about 15% upon 72 h incubation. These results are comparable to control cells (cells that have not been exposed to SWCNTs) and they emphasize that user-controlled acids oxidation time can be employed to create a library of sample of SWCNTs that have high biocompatibility with cellular system. We hypothesized that the observed trend is due to the changes in the chemical and physical structure of the SWCNTs upon acid functionalization. Specifically, shorter and more hydrophilic SWCNTs (see our previous EDX and AFM results) would be predominantly taken up by the cells through endocytosis [60], while for the longer SWCNTs the uptake mechanism is predominantly through piercing [61]. Further, the longer SWCNTs once taken up by the cells can localize at the cell nucleus and interfere with the normal progression of cells to

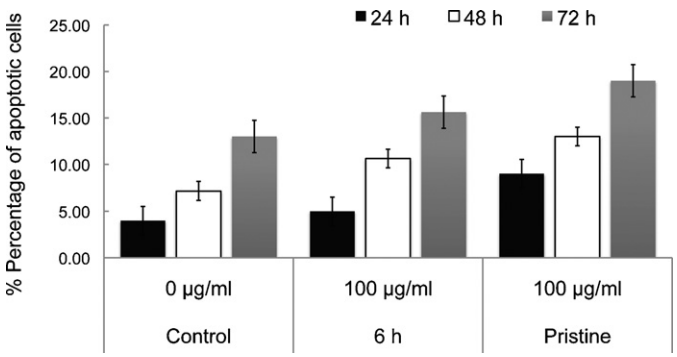

Fig. 6. Cytotoxicity of pristine and 6 h acids treated SWCNTs to BEAS-2B human epithelial cells after 24, 48 and 72 h, respectively.

Table 2
Loading and retained specific activity of immobilized SBP onto acids treated MWCNTs.

Sample	Loading (mg SBP/mg MWCNTs)	Retained specific activity (%)
1 h cut covalent	0.254 ± 0.05	9.40 ± 1.68
3 h cut covalent	0.282 ± 0.06	28.18 ± 6.52
6 h cut covalent	0.265 ± 0.15	33.97 ± 9.82

division [58,60] thus leading to the observed results. In the future, such library can be utilized for instance for the cellular delivery of drugs or molecules of interest [11].

Secondly, we tested the biocompatibility of the CNTs in relation to enzyme immobilization. Enzyme immobilization provides enzyme reutilization and eliminates costly enzyme recovery and purification processes. CNTs have high surface area [62] that facilitates the preparation of enzyme–CNTs conjugates with high enzyme loadings per unit weight of material [63,64] and promote protein activity and stability in strongly denaturing environments [63–67]. A test enzyme, namely soybean peroxidase (SBP) was immobilized through covalent binding onto MWCNTs [64,65,68–73]. Table 2 shows the loading (defined as the amount of the enzyme immobilized onto the MWCNTs) and the retained specific activity of the enzyme after immobilization. Our results show that the physical and chemical properties of the CNTs influence the enzyme loading and retained specific activity. The lowest activity was observed for the SBP immobilized onto the 1 h acids treated MWCNTs, while the activity of SBP immobilized onto 3 and 6 h acids treated MWCNTs showed similar values. The lower activity observed for the SBP immobilized onto 1 h acids oxidized MWCNTs can be attributed to the lower solubility of these CNTs (see Fig. 4b). Specifically, lower solubility of the MWCNTs leads to larger conglomerate formation (due to predominant van der Waals interactions between the MWCNTs hydrophobic walls) thus resulting in a lower surface area exposed for immobilization of SBP. Further, SBP (a 40 kDa molecular weight enzyme) has an isoelectric point of 3.9 [74]; thus, at the working PBS's pH, the protein will have a negative charge which will lead to stronger interactions with the more hydrophobic substrates of 1 h acids treated MWCNTs when compared to the less hydrophobic 3 and 6 h acids oxidized samples. Stronger binding of the SBP to the substrate will further lead to a reduction in the protein activity [32,74]. Such example demonstrated the utility of creating biocompatible MWCNTs nanosupports for biosensors applications [10]; such enzyme-nanosupport-based application can further be employed for decontamination of bacteria and spores [32].

4. Conclusion

Our results have shown that user-controlled acid oxidation of CNTs led to the formation of a library of samples with different physical and chemical properties. Specifically, we have shown that CNTs oxidation with a nitric and sulfuric acids mixture results in removal of metal catalyst, an increase in the number of functional groups having electron accepting ability, and generation of shorter CNTs with higher solubility in aqueous environments. Our results were confirmed by Raman spectroscopy, SEM, AFM, EDX and solubility tests. Further, we have shown that CNTs acids oxidation improves nanotube biocompatibility as tested by direct incubation with human epithelial cells or with test enzymes. User-controlled design of CNTs biocompatibility can lead to new types of analytical tools for life science and biotechnology [75–77].

Acknowledgements

This work is support by the NSF/CBET 1033266 and NSF/EPS-1003907. The authors acknowledge Adrienne McGraw, Chemical Engineering/WVU for her help with EDX/SEM analysis and Dr. Weiqiang Ding/WVNano for his help with Raman analysis. Authors acknowledge use of the WVU Shared Research Facilities.

References

[1] F.F. Shao, T.W. Ng, J. Fu, W. Shen, W.Y.L. Ling, Electrical circuits from capillary flow driven evaporation deposition of carbon nanotube ink in non-porous V-grooves, J. Colloid Interf. Sci. 363 (2011) 425–430.
[2] A. Nikitin, X.L. Li, Z.Y. Zhang, H. Ogasawara, H.J. Dai, A. Nilsson, Hydrogen storage in carbon nanotubes through the formation of stable C—H bonds, Nano Lett. 8 (2008) 162–167.
[3] A. Cusano, M. Consales, A. Crescitelli, M. Penza, P. Aversa, C.D. Veneri, M. Giordano, Charge transfer effects on the sensing properties of fiber optic chemical nano-sensors based on single-walled carbon nanotubes, Carbon 47 (2009) 782–788.
[4] M.H.A. Ng, L.T. Hartadi, H. Tan, C.H.P. Poa, Efficient coating of transparent and conductive carbon nanotube thin films on plastic substrates, Nanotechnology 19 (2008).
[5] B.D. Holt, K.N. Dahl, M.F. Islam, Cells take up and recover from protein-stabilized single-wall carbon nanotubes with two distinct rates, ACS Nano 6 (2012) 3481–3490.
[6] C.Z. Dinu, S.S. Bale, D.B. Chrisey, J.S. Dordick, Manipulation of individual carbon nanotubes by reconstructing the intracellular transport of a living cell, Adv. Mater. 21 (2009) 1182–1186.
[7] C.Z. Dinu, I.V. Borkar, S.S. Bale, A.S. Campbell, R.S. Kane, J.S. Dordick, Perhydrolase-nanotube-paint sporicidal composites stabilized by intramolecular crosslinking, J. Mol. Catal. B—Enzym. 75 (2012) 20–26.
[8] H. Chen, J. Wang, G. Liang, P. Zhang, J. Kong, A novel exonuclease III aided amplification method for sensitive nucleic acid detection based on single walled carbon nanotube induced quenching, Chem. Commun. 48 (2012) 269–271.
[9] D.A. Ho, Beyond the sparkle: the impact of nanodiamonds as biolabeling and therapeutic agents, ACS Nano 3 (2009) 3825–3829.
[10] J.C. Claussen, A.D. Franklin, A. ul Haque, D.M. Porterfield, T.S. Fisher, Electrochemical biosensor of nanocube-augmented carbon nanotube networks, ACS Nano 3 (2009) 37–44.
[11] A.A. Bhirde, V. Patel, J. Gavard, G.F. Zhang, A.A. Sousa, A. Masedunskas, R.D. Leapman, R. Weigert, J.S. Gutkind, J.F. Rusling, Targeted killing of cancer cells in vivo and in vitro with EGF-directed carbon nanotube-based drug delivery, ACS Nano 3 (2009) 307–316.
[12] C. Fernandez-Sanchez, E. Pellicer, J. Orozco, C. Jimenez-Jorquera, L.M. Lechuga, E. Mendoza, Plasma-activated multi-walled carbon nanotube-polystyrene composite substrates for biosensing, Nanotechnology 20 (2009).
[13] G. Cellot, E. Cilia, S. Cipollone, V. Rancic, A. Sucapane, S. Giordani, L. Gambazzi, H. Markram, M. Grandolfo, D. Scaini, F. Gelain, L. Casalis, M. Prato, M. Giugliano, L. Ballerini, Carbon nanotubes might improve neuronal performance by favouring electrical shortcuts, Nat. Nanotechnol. 4 (2009) 126–133.
[14] L.L. Ji, Y. Shao, Z.Y. Xu, S.R. Zheng, D.Q. Zhu, Adsorption of monoaromatic compounds and pharmaceutical antibiotics on carbon nanotubes activated by KOH etching, Environ. Sci. Technol. 44 (2010) 6429–6436.
[15] Y. Kimura, J.A. Nuth, N.M. Johnson, K.D. Farmer, K.P. Roberts, S.R. Hussaini, Synthesis of stacked-cup carbon nanotubes in a metal free low temperature system, Nanosci. Nanotechnol. Lett. 3 (2011) 4–10.
[16] M. Amer, A. Bushmaker, S. Cronin, Anomalous kink behavior in the current–voltage characteristics of suspended carbon nanotubes, Nano Res. 5 (2012) 172–180.
[17] J.J. Vilatela, J.A. Elliott, A.H. Windle, A model for the strength of yarn-like carbon nanotube fibers, ACS Nano 5 (2011) 1921–1927.
[18] L.M. Sargent, A.F. Hubbs, S.H. Young, M.L. Kashon, C.Z. Dinu, J.L. Salisbury, S.A. Benkovic, D.T. Lowry, A.R. Murray, E.R. Kisin, K.J. Siegrist, L. Battelli, J. Mastovich, J.L. Sturgeon, K.L. Bunker, A.A. Shvedova, S.H. Reynolds, Single-walled carbon nanotube-induced mitotic disruption, Mutat. Res. Genet. Toxicol. Environ. Mutagen 745 (2012) 28–37.
[19] S. Zhang, T. Shado, S.S. Bekaroglu, T. Karanfil, The impacts of aggregation and surface chemistry of carbon nanotubes on the adsorption of synthetic organic compounds, Environ. Sci. Technol. 43 (2009) 5719–5725.
[20] K.A. Wepasnick, B.A. Smith, K.E. Schrote, H.K. Wilson, S.R. Diegelmann, D.H. Fairbrother, Surface and structural characterization of multi-walled carbon nanotubes following different oxidative treatments, Carbon 49 (2011) 24–36.
[21] D.H. Marsh, G.A. Rance, M.H. Zaka, R.J. Whitby, A.N. Khlobystov, Comparison of the stability of multiwalled carbon nanotube dispersions in water, Phys. Chem. Chem. Phys. 9 (2007) 5490–5496.
[22] A.E. Porter, M. Gass, J.S. Bendall, K. Muller, A. Goode, J.N. Skepper, P.A. Midgley, M. Welland, Uptake of noncytotoxic acid-treated single-walled carbon nanotubes into the cytoplasm of human macrophage cells, Acs Nano 3 (2009) 1485–1492.
[23] J.G. Park, S. Li, R. Liang, C. Zhang, B. Wang, Structural changes and Raman analysis of single-walled carbon nanotube buckypaper after high current density induced burning, Carbon 46 (2008) 1175–1183.

[24] W. Guo, Z.P. Dou, H. Li, Z.J. Shi, H.F. Sun, Y.F. Liu, An efficient strategy for the purification of cloth-like single walled carbon nanotube soot produced by arc discharge, Carbon 48 (2010) 3769–3777.
[25] Z.H. Qu, G.J. Wang, Effective chemical oxidation on the structure of multiwalled carbon nanotubes, J. Nanosci. Nanotechnol. 12 (2012) 105–111.
[26] L.X. Li, F. Li, The effect of carbonyl, carboxyl and hydroxyl groups on the capacitance of carbon nanotubes, New Carbon Mater. 26 (2011) 224–228.
[27] L.F. Chen, H.Q. Xie, Y. Li, A. Yu, Surface chemical modification of multiwalled carbon nanotubes by a wet-mechanochemical reaction, J. Nanomater. 2008 (2008) 1–5, Article ID 783981.
[28] Y.R. Shin, I.Y. Jeon, J.B. Baek, Stability of multi-walled carbon nanotubes in commonly used acidic media, Carbon 50 (2012) 1465–1476.
[29] B. Smith, K. Wepasnick, K.E. Schrote, A.H. Bertele, W.P. Ball, C. O'Melia, D.H. Fairbrother, Colloidal properties of aqueous suspensions of acid-treated, multiwalled carbon nanotubes, Environ. Sci. Technol. 43 (2009) 819–825.
[30] V. Georgakilas, A. Bourlinos, D. Gournis, T. Tsoufis, C. Trapalis, A. Mateo-Alonso, M. Prato, Multipurpose organically modified carbon nanotubes: from functionalization to nanotube composites, J. Am. Chem. Soc. 130 (2008) 8733–8740.
[31] V. Datsyuk, M. Kalyva, K. Papagelis, J. Parthenios, D. Tasis, A. Siokou, I. Kallitsis, C. Galiotis, Chemical oxidation of multiwalled carbon nanotubes, Carbon 46 (2008) 833–840.
[32] C.Z. Dinu, G. Zhu, S.S. Bale, G. Anand, P.J. Reeder, K. Sanford, G. Whited, R.S. Kane, J.S. Dordick, Enzyme-based nanoscale composites for use as active decontamination surfaces, Adv. Funct. Mater. 20 (2010) 392–398.
[33] N.E. Marks, A.S. Grandison, M.J. Lewis, Challenge testing of the lactoperoxidase system in pasteurized milk, J. Appl. Microbiol. 91 (2001) 735–741.
[34] G.A. Forrest, A.J. Alexander, A model for the dependence of carbon nanotube length on acid oxidation time, J. Phys. Chem. C 111 (2007) 10792–10798.
[35] M.A. Hamon, H. Hu, P. Bhowmik, S. Niyogi, B. Zhao, M.E. Itkis, R.C. Haddon, End-group, defect analysis of soluble single-walled carbon nanotubes, Chem. Phys. Lett. 347 (2001) 8–12.
[36] H. Hu, P. Bhowmik, B. Zhao, M.A. Hamon, M.E. Itkis, R.C. Haddon, Determination of the acidic sites of purified single-walled carbon nanotubes by acid–base titration, Chem. Phys. Lett. 345 (2001) 25–28.
[37] M.W. Marshall, S. Popa-Nita, J.G. Shapter, Measurement of functionalised carbon nanotube carboxylic acid groups using a simple chemical process, Carbon 44 (2006) 1137–1141.
[38] N. Kulshrestha, A. Misra, K.S. Hazra, S. Roy, R. Bajpai, D.R. Mohapatra, D.S. Misra, Healing of broken multiwalled carbon nanotubes using very low energy electrons in SEM: a route toward complete recovery, ACS Nano 5 (2011) 1724–1730.
[39] R. Kozhuharova, M. Ritschel, D. Elefant, A. Graff, A. Leonhardt, I. Monch, T. Muhl, C.M. Schneider, Synthesis and characterization of aligned Fe-filled carbon nanotubes on silicon substrates, J. Mater. Sci.—Mater. Electron. 14 (2003) 789–791.
[40] A. Hirano, T. Tanaka, Y. Urabe, H. Kataura, Purification of single-wall carbon nanotubes by controlling the adsorbability onto agarose gels using deoxycholate, J. Phys. Chem. C 116 (2012) 9816–9823.
[41] A.R. Biris, L.P. Dan, E. Dervishi, Z.R. Li, Y. Xu, S. Trigwell, I. Misan, A.S. Biris, Multiwall carbon nanotubes synthesized by RF-CCVD on novel CaO supported catalysts, Phys. Lett. A 372 (2008) 6416–6419.
[42] M.S. Dresselhaus, A. Jorio, M. Hofmann, G. Dresselhaus, R. Saito, Perspectives on carbon nanotubes and graphene Raman spectroscopy, Nano Lett. 10 (2010) 751–758.
[43] A.K. Mishra, S. Ramaprabhu, Nano magnetite decorated multiwalled carbon nanotubes: a robust nanomaterial for enhanced carbon dioxide adsorption, Energ. Environ. Sci. 4 (2011) 889–895.
[44] C.B. Dong, Z.J. Yan, J. Kokx, C.Z. Dinu, D.B. Chrisey, Antibacterial and surface-enhanced Raman scattering (SERS) activities of AgCl cubes synthesized by pulsed laser ablation in liquid, Appl. Surf. Sci. 258 (2012) 9218–9222.
[45] J. Maultzsch, S. Reich, C. Thomsen, S. Webster, R. Czerw, D.L. Carroll, S.M.C. Vieira, P.R. Birkett, C.A. Rego, Raman characterization of boron-doped multiwalled carbon nanotubes, Appl. Phys. Lett. 81 (2002) 2647–2649.
[46] E. Dervishi, Z. Li, A.R. Biris, D. Lupu, S. Trigwell, A.S. Biris, Morphology of multi-walled carbon nanotubes affected by the thermal stability of the catalyst system, Chem. Mater. 19 (2007) 179–184.
[47] C.W. Yang, X.U. Hu, Y. Zhang, A study of the functionalization on multi-walled carbon nanotubes, in: 2006 1st IEEE International Conference on Nano/Micro Engineered and Molecular Systems, vols. 1–3, 2006, pp. 83–86.
[48] M. Kalbac, Y.P. Hsieh, H. Farhat, L. Kavan, M. Hofmann, J. Kong, M.S. Dresselhaus, Defects in individual semiconducting single wall carbon nanotubes: Raman spectroscopic and in situ Raman spectroelectrochemical study, Nano Lett. 10 (2010) 4619–4626.
[49] S. Dittmer, N. Olofsson, J.E. Weis, O.A. Nerushev, A.V. Gromov, E.E.B. Campbell, In situ Raman studies of single-walled carbon nanotubes grown by local catalyst heating, Chem. Phys. Lett. 457 (2008) 206–210.
[50] K.A. Wepasnick, B.A. Smith, J.L. Bitter, D.H. Fairbrother, Chemical and structural characterization of carbon nanotube surfaces, Anal. Bioanal. Chem. 396 (2010) 1003–1014.
[51] L. Shao, G. Tobias, C.G. Salzmann, B. Ballesteros, S.Y. Hong, A. Crossley, B.G. Davis, M.L.H. Green, Removal of amorphous carbon for the efficient sidewall functionalisation of single-walled carbon nanotubes, Chem. Commun. (2007) 5090–5092.
[52] M.N. Tchoul, W.T. Ford, G. Lolli, D.E. Resasco, S. Arepalli, Effect of mild nitric acid oxidation on dispersability, size, and structure of single-walled carbon nanotubes, Chem. Mater. 19 (2007) 5765–5772.
[53] L.R. Gu, P.J.G. Luo, H.F. Wang, M.J. Meziani, Y. Lin, L.M. Veca, L. Cao, F.S. Lu, X. Wang, R.A. Quinn, W. Wang, P.Y. Zhang, S. Lacher, Y.P. Sun, Single-walled carbon nanotube as a unique scaffold for the multivalent display of sugars, Biomacromolecules 9 (2008) 2408–2418.
[54] Y.T. Shieh, G.L. Liu, H.H. Wu, C.C. Lee, Effects of polarity and pH on the solubility of acid-treated carbon nanotubes in different media, Carbon 45 (2007) 1880–1890.
[55] Y.T. Shieh, J.Y. Chen, Y.K. Twu, W.J. Chen, The effect of pH and ionic strength on the dispersion of carbon nanotubes in poly(acrylic acid) solutions, Polym. Int. 61 (2012) 554–559.
[56] E. Heister, C. Lamprecht, V. Neves, C. Tilmaciu, L. Datas, E. Flahaut, B. Soula, P. Hinterdorfer, H.M. Coley, S.R.P. Silva, J. McFadden, Higher dispersion efficacy of functionalized carbon nanotubes in chemical and biological environments, ACS Nano 4 (2010) 2615–2626.
[57] C. Bussy, J. Cambedouzou, S. Lanone, E. Leccia, V. Heresanu, M. Pinault, M. Mayne-l'Hermite, N. Brun, C. Mory, M. Cotte, J. Doucet, J. Boczkowski, P. Launoist, Carbon nanotubes in macrophages: imaging and chemical analysis by X-ray fluorescence microscopy, Nano Lett. 8 (2008) 2659–2663.
[58] L.M. Sargent, A.A. Shvedova, A.F. Hubbs, J.L. Salisbury, S.A. Benkovic, M.L. Kashon, D.T. Lowry, A.R. Murray, E.R. Kisin, S. Friend, K.T. McKinstry, L. Battelli, S.H. Reynolds, Induction of aneuploidy by single-walled carbon nanotubes, Environ. Mol. Mutagen 50 (2009) 708–717.
[59] A.D. Maynard, P.A. Baron, M. Foley, A.A. Shvedova, E.R. Kisin, V. Castranova, Exposure to carbon nanotube material: aerosol release during the handling of unrefined single-walled carbon nanotube material, J. Toxicol. Environ. Health Part A 67 (2004) 87–107.
[60] H. Jin, D.A. Heller, R. Sharma, M.S. Strano, Size-dependent cellular uptake and expulsion of single-walled carbon nanotubes: single particle tracking and a generic uptake model for nanoparticles, ACS Nano 3 (2009) 149–158.
[61] S. Pogodin, V.A. Baulin, Can a carbon nanotube pierce through a phospholipid bilayer? ACS Nano 4 (2010) 5293–5300.
[62] S. Chakraborty, J. Chattopadhyay, H. Peng, Z. Chen, A. Mukherjee, R.S. Arvidson, R.H. Hauge, W.E. Billups, Surface area measurement of functionalized single-walled carbon nanotubes, J. Phys. Chem. B 110 (2006) 24812–24815.
[63] P. Asuri, S.S. Karajanagi, A.A. Vertegel, J.S. Dordick, R.S. Kane, Enhanced stability of enzymes adsorbed onto nanoparticles, J. Nanosci. Nanotechnol. 7 (2007) 1675–1678.
[64] P. Asuri, S.S. Karajanagi, H. Yang, T.J. Yim, R.S. Kane, J.S. Dordick, Increasing protein stability through control of the nanoscale environment, Langmuir 22 (2006) 5833–5836.
[65] S.S. Karajanagi, H. Yang, P. Asuri, E. Sellitto, J.S. Dordick, R.S. Kane, Protein-assisted solubilization of single-walled carbon nanotubes, Langmuir 22 (2006) 1392–1395.
[66] M.A. Alonso-Lomillo, O. Ruediger, A. Maroto-Valiente, M. Velez, I. Rodriguez-Ramos, F.J. Munoz, V.M. Fernandez, A.L. De Lacey, Hydrogenase-coated carbon nanotubes for efficient H_2 oxidation, Nano Lett. 7 (2007) 1603–1608.
[67] X. Yu, D. Chattopadhyay, I. Galeska, F. Papadimitrakopoulos, J.F. Rusling, Peroxidase activity of enzymes bound to the ends of single-wall carbon nanotube forest electrodes, Electrochem. Commun. 5 (2003) 408–411.
[68] P. Asuri, S.S. Bale, S.S. Karajanagi, R.S. Kane, The protein–nanomaterial interface, Curr. Opin. Biotechnol. 17 (2006) 562–568.
[69] P. Asuri, S.S. Karajanagi, E. Sellitto, D.Y. Kim, R.S. Kane, J.S. Dordick, Water-soluble carbon nanotube–enzyme conjugates as functional biocatalytic formulations, Biotechnol. Bioeng. 95 (2006) 804–811.
[70] P. Asuri, S.S. Karajanagi, J.S. Dordick, R.S. Kane, Directed assembly of carbon nanotubes at liquid–liquid interfaces: nanoscale conveyors for interfacial biocatalysis, J. Am. Chem. Soc. 128 (2006) 1046–1047.
[71] K.A. Joshi, J. Tang, R. Haddon, J. Wang, W. Chen, A. Mulchandani, A disposable biosensor for organophosphorus nerve agents based on carbon nanotubes modified thick film strip electrode, Electroanalysis 17 (2005) 54–58.
[72] J. Li, Y.-B. Wang, J.-D. Qiu, D.-C. Sun, X.-H. Xia, Biocomposites of covalently linked glucose oxidase on carbon nanotubes for glucose biosensor, Anal. Bioanal. Chem. 383 (2005) 918–922.
[73] N. Jia, L. Liu, Q. Zhou, L. Wang, M. Yan, Z. Jiang, Bioelectrochemistry and enzymatic activity of glucose oxidase immobilized onto the bamboo-shaped CN*x* nanotubes, Electrochim. Acta 51 (2005) 611–618.
[74] W.C. Zhang, X.H. Dai, Y. Zhao, X.M. Lu, P.J. Gao, Comparison of the different types of surfactants for the effect on activity and structure of soybean peroxidase, Langmuir 25 (2009) 2363–2368.
[75] Y. Lin, S. Taylor, H. Li, K.A.S. Fernando, L. Qu, W. Wang, L. Gu, B. Zhou, Y.-P. Sun, Advances toward bioapplications of carbon nanotubes, J. Mater. Chem. 14 (2004) 527–541.
[76] Y.P. Sun, K. Fu, Y. Lin, W. Huang, Functionalized carbon nanotubes: properties and applications, Acc. Chem. Res. 35 (2002) 1096–1104.
[77] R.H. Baughman, A.A. Zakhidov, W.A. de Heer, Carbon nanotubes—the route toward applications, Science 297 (2002) 787–792.